AD-A036 473 CONSTRUCTION ENGINEERING RESEARCH LAB (ARMY) CHAMPAI--ETC F/G 20/11
A PLASTICITY FORMULATION FOR CYCLIC INELASTIC STRUCTURAL ANALYS--ETC(U)
FEB 77 S K SHARMA, H R JHANSALE

UNCLASSIFIED CERL-IR-M-202 NL

1 OF 1
ADA036473

END

DATE
FILMED
3-77

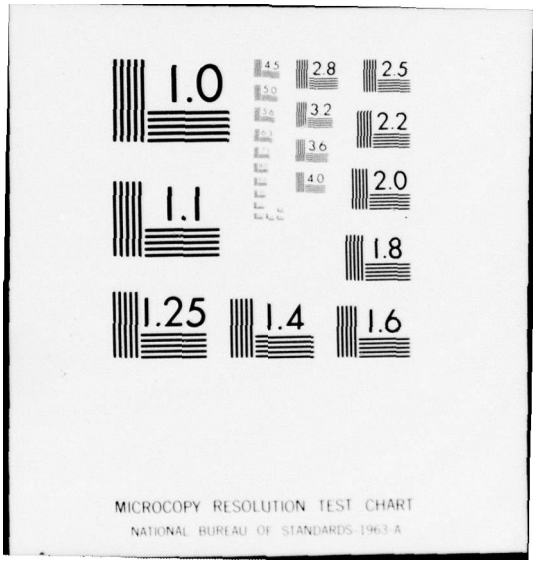
1.0
1.1
1.25
1.4
1.6
1.8
2.0
2.2
2.5
2.8
3.2
3.6
4.0
4.5
5.0
MICROCOPY RESOLUTION TEST CHART
NATIONAL BUREAU OF STANDARDS-1963-A

construction
engineering
research
laboratory

INTERIM REPORT M-202
February 1977

A PLASTICITY FORMULATION FOR CYCLIC INELASTIC STRUCTURAL ANALYSIS

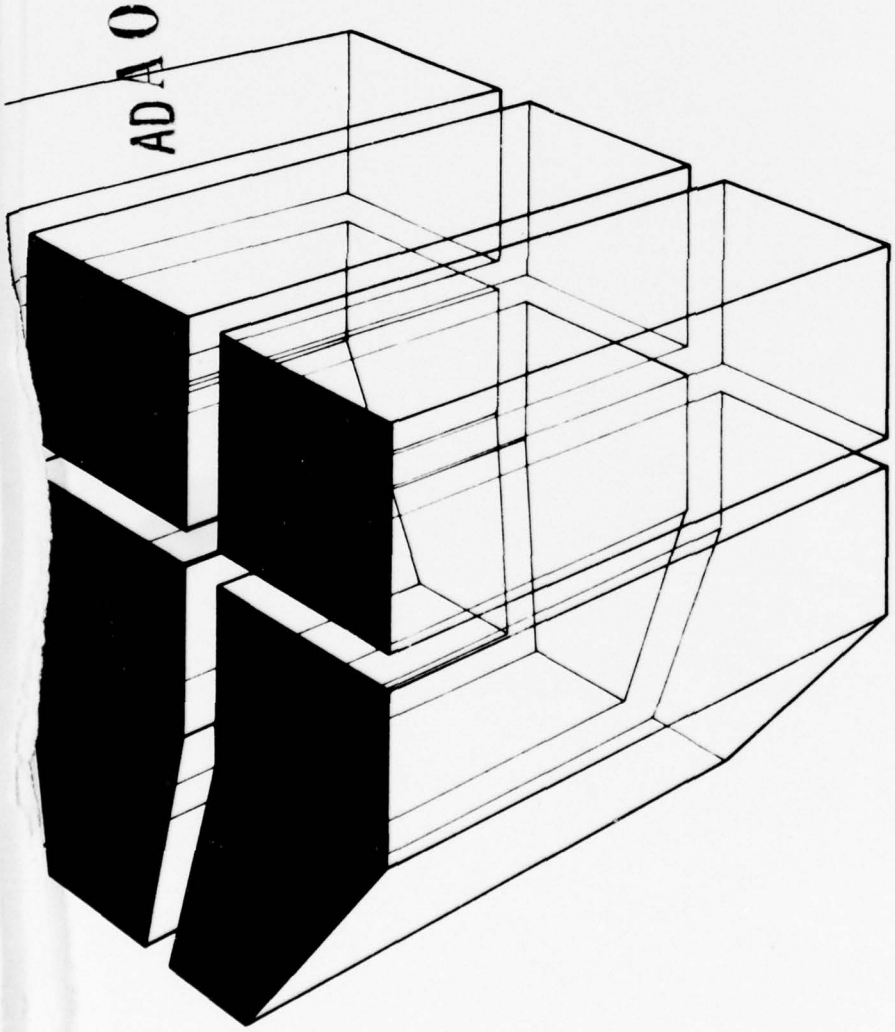

by
S. K. Sharma
H. R. Jhansale

The contents of this report are not to be used for advertising, publication, or promotional purposes. Citation of trade names does not constitute an official indorsement or approval of the use of such commercial products. The findings of this report are not to be construed as an official Department of the Army position, unless so designated by other authorized documents.

DESTROY THIS REPORT WHEN IT IS NO LONGER NEEDED
DO NOT RETURN IT TO THE ORIGINATOR

UNCLASSIFIED

SECURITY CLASSIFICATION OF THIS PAGE *(When Data Entered)*

REPORT DOCUMENTATION PAGE

READ INSTRUCTIONS BEFORE COMPLETING FORM

1. REPORT NUMBER: INTERIM REPORT M-202
2. GOVT ACCESSION NO.
3. RECIPIENT'S CATALOG NUMBER

4. TITLE (and Subtitle): A PLASTICITY FORMULATION FOR CYCLIC INELASTIC STRUCTURAL ANALYSIS.
5. TYPE OF REPORT & PERIOD COVERED: INTERIM rept.
6. PERFORMING ORG. REPORT NUMBER

7. AUTHOR(s): S. K. Sharma, H. R. Ohansale
8. CONTRACT OR GRANT NUMBER(s)

9. PERFORMING ORGANIZATION NAME AND ADDRESS:
CONSTRUCTION ENGINEERING RESEARCH LABORATORY
P.O. Box 4005
Champaign, Illinois 61820

10. PROGRAM ELEMENT, PROJECT, TASK AREA & WORK UNIT NUMBERS: 4A161102AT23-02-004

11. CONTROLLING OFFICE NAME AND ADDRESS

12. REPORT DATE: February 1977
13. NUMBER OF PAGES: 27

14. MONITORING AGENCY NAME & ADDRESS *(if different from Controlling Office)*: 28p.
15. SECURITY CLASS. *(of this report)*: UNCLASSIFIED
15a. DECLASSIFICATION/DOWNGRADING SCHEDULE

16. DISTRIBUTION STATEMENT *(of this Report)*

Approved for public release; distribution unlimited. 02

CERL-IR-M-202

17. DISTRIBUTION STATEMENT *(of the abstract entered in Block 20, if different from Report)*

18. SUPPLEMENTARY NOTES

Copies are obtainable from National Technical Information Service, Springfield, VA 22151

19. KEY WORDS *(Continue on reverse side if necessary and identify by block number)*

inelastic structural analysis
plasticity formulation
cyclic analysis

20. ABSTRACT *(Continue on reverse side if necessary and identify by block number)*

A critical review of current inelastic structural analysis procedures indicates that the material constitutive models presently in use do not adequately reflect the materials' cyclic inelastic properties. This will result in erroneous evaluation of deformation response and energy dissipation in structures subjected to dynamic loadings.

This report presents a plasticity formulation which is capable of simulating all the important features of material properties observed under cyclic uniaxial loading.

DD FORM 1 JAN 73 1473 EDITION OF 1 NOV 65 IS OBSOLETE 405 272 UNCLASSIFIED

SECURITY CLASSIFICATION OF THIS PAGE *(When Data Entered)*

Appropriate cyclic material properties required for characterizing the combined isotropic-kinematic hardening features of this formulation are defined. These properties are determined from simple cyclic uniaxial tests. The formulation uses Mroz's concept of multiple and nesting hypersurfaces in stress space to simulate the memory of prior history; it eliminates the need for classifying a general loading path into a plastic loading or a plastic load reversal for cyclic analysis. The superiority of this formulation over currently available methods is demonstrated.

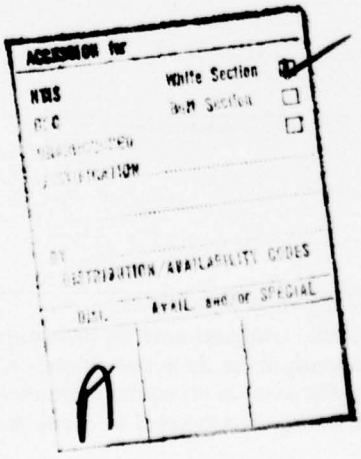

FOREWORD

This investigation was conducted for the Directorate of Military Construction, Office of the Chief of Engineers (OCE) by the Structural Mechanics Branch (MSS), Materials and Science Division (MS), Construction Engineering Research Laboratory (CERL). The project was a part of the RDT&E Army Program 6.27.19-A, Project 4A161102AT23, "Research in Military Engineering and Construction"; Task 02, "Analytical and Theoretical Studies of Complex Structural Systems"; Work Unit 004, "Energy Dissipation in Dynamically Loaded Structures." The OCE Technical Monitor was Mr. George Matsumura.

The assistance of Dr. W. E. Fisher, Chief of MSS, is acknowledged. Dr. G. R. Williamson is Chief of MS, COL J. E. Hays is Commander and Director of CERL, and Dr. L. R. Shaffer is Technical Director.

CONTENTS

LIST OF FIGURES

A PLASTICITY FORMULATION FOR CYCLIC INELASTIC STRUCTURAL ANALYSIS

1 INTRODUCTION

Background

A structure's energy absorption capacity is important to its safety during dynamic loading such as that occurring during an earthquake. Inelastic hysteretic deformation is a major source of energy dissipation in structures under such loadings. Therefore, estimates of energy dissipation should be based on an inelastic deformation analysis appropriate to cyclic loading conditions. Such an analysis would be useful for evaluating plastic structural design procedures as well as inelastic instability and cumulative fatigue damage criteria. Inelastic analyses and design procedures will also help achieve safe and economical structures through effective use of their strengths in the inelastic range.

A review of current structural analysis procedures and plasticity formulation indicates that the material constitutive equations (multiaxial stress-strain relationships) used in these procedures do not adequately represent material characteristics under cyclic loading. Using such an analysis would cause serious errors in estimating energy dissipation, ductility, and inelastic deformation.

Extensive low-cycle fatigue research during the past two decades has provided considerable insight into various plastic hysteresis phenomena and cyclic history dependence of the uniaxial stress-strain behavior of metals. Based on these findings, a unified approach of characterizing the cyclic uniaxial properties has been developed.[1] Sufficient experimental data on cyclic material characteristics under multi-axial stress states are not yet available. Therefore, the only feasible approach is to develop a formulation within the framework of the established classical theory of plasticity, which can simulate the salient cyclic uniaxial material characteristics.

Purpose

The purpose of this report is to present a plasticity formulation for structural materials that adequately represents all the important cyclic material properties and that can be readily incorporated into existing finite element nonlinear structural analysis computer codes.

Approach

A previous CERL report[2] extended a cyclic uniaxial stress-strain model to the generalized state of stress by defining an equivalence between the two states. One problem with this approach was the necessity of reducing a general nonproportional loading path into only two events (loading and unloading) to define load reversals.

This problem has been eliminated in this report by adopting a different approach based on Mroz's concept of multiple and nesting hardening surfaces.[3] The translational and dilatational properties of these surfaces are determined from a set of cyclic uniaxial properties developed by Jhansale.[4] The inelastic deformation analysis using this formulation should help achieve an accurate and reliable evaluation of structural response under dynamic loading.

2 LITERATURE REVIEW

Many recently proposed mathematical models[5-7] describe deformation of materials in the inelastic range. However, for rate-insensitive materials, only the classical theory of plasticity and its various modifications have been used successfully in general structural analysis. This is due to their relative mathematical simplicity and their ability to simulate actual material behavior at least under monotonic loadings. The classical theory of plasticity with a constant yield surface (perfect plasticity model) or a monotonically expanding yield surface (isotropic

[1] H. R. Jhansale, "A Friction Stress Method for the Cyclic Inelastic Behavior of Metals," *Transactions of the 3rd International Conference on Structural Mechanics in Reactor Technology*, Vol 5, Paper L5/4 (1975).

[2] J. F. McNamara and S. K. Sharma, *Isotropic-Kinematic Hardening Model for Elastic-Plastic Structural Analysis*, Technical Report M-148/ADA014945 (Construction Engineering Research Laboratory [CERL], August, 1975).

[3] Z. Mroz, "An Attempt to Describe the Behavior of Metals Under Cyclic Loads Using a More General Workhardening Model," *Acta Mechanica*, Vol 7, No. 2-3 (1969), pp 199-212.

[4] Jhansale, "A Friction Stress Method for the Cyclic Inelastic Behavior of Metals."

[5] J. R. Rice, "On the Structure of Stress-Strain Relations for Time-Dependent Plastic Deformation of Metals," *Journal of Applied Mechanics*, Vol 37 (1970), pp 728-737.

[6] T. Mura, "Continuum Theory of Dislocations and Plasticity," *Mechanics of Generalized Continua*, E. Kroner, ed. (Springer-Verlag, 1968), pp 269-278.

[7] K. C. Valanis, "A Theory of Viscoplasticity Without a Yield Surface," *Archives Mechanics*, Vol 23 (1971), pp 517-551.

hardening model) has been presented in detail.[8,9] A constant or expanding yield surface conflicts with the experimental Baushinger effect phenomenon, which is denoted by a reduced yield strength after a stress reversal following plastic straining. To simulate the Baushinger effect, Prager[10] introduced a kinematic hardening model in which yield surface translates without rotation or distortion in the direction of plastic strain increments. This kinematic hardening model was modified by Ziegler[11] to make translation of the yield surface invariant under a reduction of the dimension of stress space.

The use of the classical plasticity theory with isotropic or kinematic hardening models requires a material constant which is usually determined from an experimental uniaxial stress-strain curve. A correspondence is established between multiaxial and uniaxial stress-strain paths by defining equivalent increment of plastic strain from multiaxial plastic strain increments. The material constant is then determined from the slope of the experimental uniaxial stress-strain curve at a point which corresponds to current stress state for the multiaxial case. This approach for determining the material constant experiences several difficulties when cyclic plastic deformations are involved. If only a monotonic experimental uniaxial curve is used, then multiaxial plastic strains in any direction, including the completely reversed direction, must be reduced to a monotonically increasing plastic strain. If reverse plastic straining for the uniaxial curve is also permitted, then every increment of multiaxial plastic deformation must be defined as a case of either loading or reversed loading. There is no smooth transition from a case of continued loading to a case of completely reversed loading. Moreover, an analytical model for generating cyclic uniaxial stress-strain must be formulated. This curve cannot be obtained experimentally because the history of deformation is not known *a priori.*

A definition for determining loading or reversed loading from multiaxial plastic deformation and a rheological material model for steel have been used in the application of the kinematic hardening theory.[12] A similar procedure for a combined isotropic-kinematic hardening theory has been used where a method to determine another material constant for isotropic hardening is also given.[13] Recently, a multiaxial plastic deformation in any direction has been considered as a case of either continued loading, partially reversed loading, or fully reversed loading.[14] A cyclic uniaxial curve has been represented by branches of a Ramberg-Osgood curve,[15] which is essentially a power law relationship between stresses and strains. The three material parameters of this curve are adjusted according to a scalar product of previous and current normal vectors in the direction of deformation.

A more consistent theory which can account for the directional dependence of reversed multiaxial plastic deformation has been proposed by Iwan[16] and by Mroz.[17] In Mroz's model, a uniaxial stress-strain curve of an initially isotropic material is approximated by piecewise linear segments of constant tangent plastic moduli. In a stress space, this approximation is represented by concentric and similar hypersurfaces defining regions of constant plastic tangent moduli. The first of these surfaces is the conventional yield surface. The yield surface translates during plastic deformation, coming in contact with and then pushing larger hypersurfaces. Motions of these surfaces are governed by the conditions that they preserve their orientations and that no two surfaces can intersect each other. These conditions give rise to a kinematic hardening rule that differs from those of Prager[18] and Ziegler.[19]

---

[8]W. Prager and P. G. Hodge, *Theory of Perfectly Plastic Solids* (John Wiley, 1951).

[9]R. Hill, *The Mathematical Theory of Plasticity* (Oxford, 1950).

[10]W. Prager, "A New Method of Analyzing Stresses and Strains in Work-Hardening Plastic Solids," *Journal of Applied Mechanics*, Vol 23 (1956), pp 493-496.

[11]H. Ziegler, "A Modification of Prager's Hardening Rule," *Quarterly of Applied Mathematics*, Vol 17 (1959), pp 55-65.

[12]F. G. Plummer, *A New Look at Structural Energy Dissipation*, Technical Report M-82/AD#780801 (CERL, May 1974).

[13]J. F. McNamara and S. K. Sharma, *Isotropic-Kinematic Hardening Model for Elastic-Plastic Structural Analysis*, Technical Report M-148/ADA014945 (CERL, August 1975).

[14]M. A. Eisenberg, "A Generalization of Plastic Flow Theory With Application to Cyclic Hardening and Softening Phenomena," *Journal of Engineering Materials and Technology*, Vol 98, Series H, No. 3 (July 1976), pp 221-228.

[15]W. Ramberg and W. R. Osgood, *Description of Stress-Strain Curves by Three Parameters*, TN 902 (National Advisory Committee for Aeronautics, 1943).

[16]W. D. Iwan, "On a Class of Models for the Yielding Behavior of Continuous and Composite Systems," *Journal of Applied Mechanics*, Vol 34 (1967), pp 612-617.

[17]Z. Mroz, "On the Description of Anisotropic Workhardening," *Journal of Mechanics of Physical Solids*, Vol 15 (1967), pp 163-175.

[18]W. Prager, "A New Method of Analyzing Stresses and Strains in Work-Hardening Plastic Solids," *Journal of Applied Mechanics*, Vol 23 (1956), pp 493-496.

[19]H. Ziegler, "A Modification of Prager's Hardening Rule," *Quarterly of Applied Mathematics*, Vol 17 (1959), pp 55-65.

Recently, Krieg[20] and Dafalias and Popov[21] have proposed a simplification of Mroz's model through consideration of only two surfaces—a yield surface which is enclosed by a limiting surface. Both of these surfaces are allowed to translate and change in size during plastic deformation. The rates of translation and the changes in size are assumed to be functions of a vector from the current stress state to a projected stress state on the limiting surface. However, Dafalias and Popov have left these functions undefined because of a lack of experimental data. Krieg has defined these functions intuitively to match experimental data for a uniaxial specimen, but their validity for multiaxial deformations has not been demonstrated. Moreover, the use of only two surfaces is inadequate for a satisfactory simulation of the "memory" effect[22] in which a material apparently remembers certain previous points of stress-strain reversals. The material exhibits discontinuities in its stress-strain response at these points on subsequent loading or unloading.

In most of the theories presented above, isotropic hardening is taken into account by changing the radius of the yield surface as a function of a monotonically increasing parameter (e.g., equivalent plastic strain, plastic work). This usually implies that the radius of the yield surface increases (or decreases) monotonically, reaching a stable value asymptotically. An obvious drawback of this approach is that the yield radius is restricted to increase (or decrease) monotonically regardless of whether the amplitude of loading cycles is increased or decreased. Once the yield radius has reached a stable value, it remains unchanged even if the amplitude of loading cycles is changed significantly. To overcome this problem, the idea of nesting hypersurfaces is extended in the formulation presented in this report to define a field of isotropic hardening moduli. All material constants required by the present approach are obtained from cyclic uniaxial experiments described briefly in Chapter 3.

[20]R. D. Krieg, "A Practical Two Surface Plasticity Theory," *Journal of Applied Mechanics*, Vol 42 (1975), pp 641-646.

[21]Y. F. Dafalias and E. P. Popov, "A Model of Nonlinearly Hardening Materials for Complex Loading," *Acta Mechanica*, Vol 21 (1975), pp 173-192.

[22]H. R. Jhansale and T. H. Topper, "An Engineering Analysis of the Inelastic Stress Response of a Structural Metal Under Variable Cyclic Strain," *Experimentation and Failure Prediction*, STP-519 (American Society for Testing and Materials, 1973).

3 CYCLIC UNIAXIAL STRESS-STRAIN BEHAVIOR

In order to meaningfully describe the cyclic uniaxial material properties, a brief outline of the plastic hysteresis phenomena of metals and a recently developed unified approach[23] for their quantitative characterization is necessary.

Transient Behavior

Cycle-dependent variations in the hysteretic behavior of metals are usually observed under constant stress- or strain-limits cycling conditions. These variations are classified as cyclic hardening, cyclic softening, cyclic creep, and cyclic relaxation. In general, these phenomena are transient, and a saturation or stable state is rapidly approached at a continuously decreasing rate with cycles. In general, materials exhibit an initial cyclic hardening or softening, depending on their initial condition and sometimes on the magnitude of the stress or strain amplitude imposed. Whenever the stress or strain limits are changed, a transient behavior ensues and a new saturation state corresponding to the new stress or strain limits is approached.

Based on the observations of a large number of structural metals of widely ranging strengths and cyclic characteristics, it has been shown[24,25] that transient behavior is essentially caused by a history-dependent variation in the material's yield strength. This variation is effected by substructural changes caused by the reversed plastic strains in the material.

Figure 1 schematically illustrates a cyclic hardening situation that compares the first three hysteresis branches. Each hysteresis branch is composed of an initial linear elastic portion and a nonlinear inelastic portion. In the case of cyclic hardening, the initial elastic portion increases in length from one branch to the next, but the elastic modulus remains unchanged. The nonlinear inelastic portions remain virtually unchanged in shape during transient behavior. The history-dependent change in the

[23]H. R. Jhansale, "A Friction Stress Method for the Cyclic Inelastic Behavior of Metals," *Transactions of the 3rd International Conference on Structural Mechanics in Reactor Technology*, Vol 5, Paper L5/4 (1975).

[24]H. R. Jhansale, "A Friction Stress Method for the Cyclic Inelastic Behavior of Metals."

[25]H. R. Jhansale, "A New Parameter for the Hysteretic Stress-Strain Behavior of Metals," *Journal of Engineering Materials and Technology*, Vol 97, No. 1 (1975), pp 33-38.

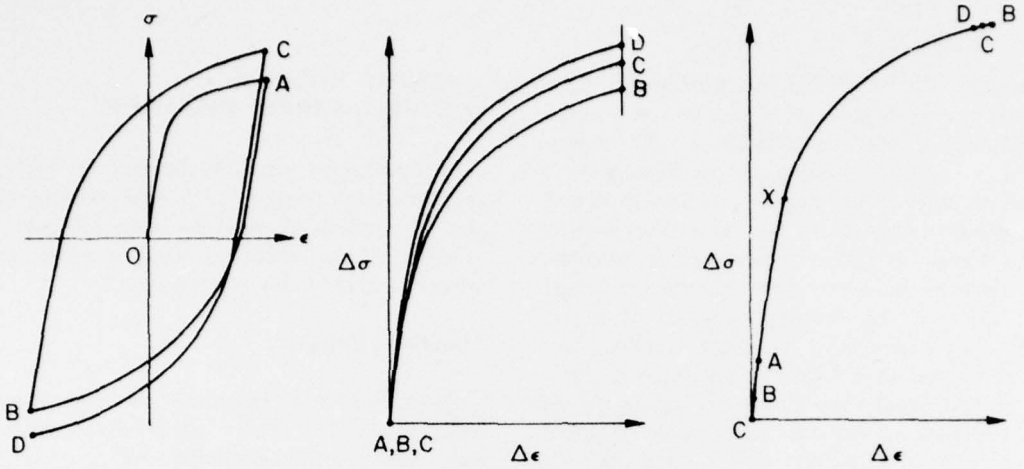

(a) Three Reversals of Cyclic Hardening.

(b) Branches AB, BC and CD are superimposed on their initial points A, B, and C, respectively.

(c) Branches AB and BC are translated along the elastic slope to match nonlinear portions.

Figure 1. Comparisons of hysteresis branches under cyclic hardening phenomenon.

linear elastic portion is termed "yield range increment" (YRI), since it represents a change in the yield strength. The invariant nonlinear inelastic portion represents an intrinsic material stress-strain characteristic that is independent of cyclic history.

Saturation Behavior

Any two consecutive hysteresis branches form a hysteresis loop. Under transient conditions, a hysteresis loop is not fully closed (Figure 1a) since its two branches are not identical. However, in the saturated state, a hysteresis loop is fully closed since the two hysteresis branches are identical, which means the yield strengths or YRIs in both branches are equal. In most metals, the saturation value of YRI is a function of the stress or strain amplitude. Based on available data, and for the purpose of engineering analysis, it is reasonable to assume that the saturation YRI is independent of prior cyclic history. Microstructural studies[26] have shown that certain types of materials develop a substructural dislocation cell size at saturation that is independent of prior history. This fact lends some support to the assumption of prior history independence of saturation YRI.

Figure 2 shows the saturation YRI plotted as a function of strain amplitude for three materials exhibiting different cyclic characteristics. The saturation YRI could also be expressed as a function of stress amplitude or plastic strain amplitude. In the case of SAE 1045 normalized steel, which exhibits cyclic softening at low strains (approximately < 0.004) and cyclic hardening at high strains, the saturation YRI increases with strain amplitude. In the case of SAE 1045 quenched and tempered steel, which cyclically softens, the saturation YRI decreases with strain amplitude. Cyclically hardening 2024-T4 aluminum is one of the few materials whose saturation YRI is independent of strain amplitude. Figure 2 shows some evidence of prior history independence of saturation YRI in the cases of SAE 1045 normalized steel and 2024-T4 aluminum.

Cyclic Uniaxial Properties

Three uniaxial material properties appropriate to the cyclic saturation state are derived from a set of hysteresis stress-strain loops corresponding to that state: cyclic stress-strain curve; skeleton stress-strain curve; and saturation yield strength increment. Such loops may be obtained from fully reversed constant strain cycling tests on multiple identical specimens, each specimen being cycled at a specified strain amplitude until saturation is achieved. Since an ideal state of saturation may never be achieved in an

[26] C. E. Felter and C. Laird, "Cyclic Stress-Strain Response of FCC Metals and Alloys," *ACTA Metallurgica*, Vol 15 (October 1967).

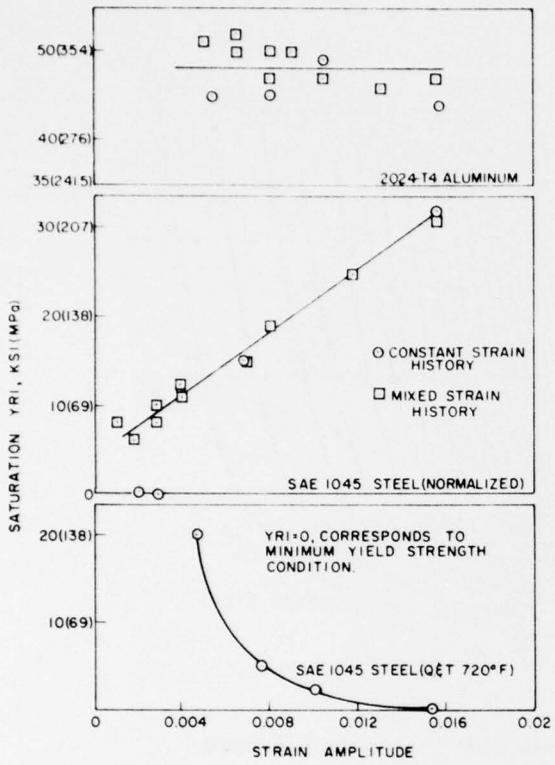

Figure 2. Saturation yield range increment for three materials.

actual test, the condition at which the transient changes are minimal may be considered to represent saturation for the present purpose. Alternatively, the saturated hysteresis loops may also be obtained in a single multi-block decremental step test as illustrated in Figure 3. In this test, the specimen is strain-cycled at a constant amplitude until saturation is achieved at that level; the sample is then tested at the next level, and so on.

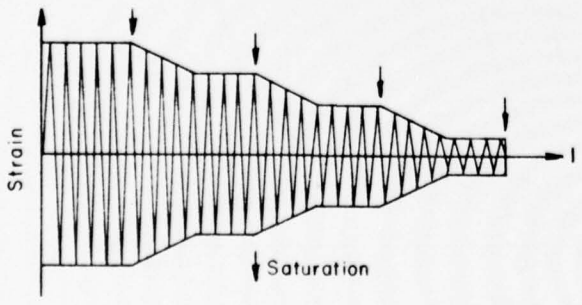

Figure 3. Strain-time history in a multi-block decremental step test.

Cyclic Stress-Strain Curve

This curve is defined as the locus of the tips of fully reversed saturated or stable hysteresis loops of various sizes (see Figure 4). The hysteresis loops shown in the figure are for A-36 steel obtained from a multiblock decremental step test. An alternative rapid method of determining the cyclic stress-strain curve by means of an "incremental step" test is described by Landgraf, et al.[27]

If the hysteresis loops are superimposed on their lower tips (Figure 5), the locus of the upper tips describes a curve that is geometrically similar to the cyclic stress-strain curve, but magnified by a scale factor of two. This relationship results from the symmetry property of the hysteresis branches.

Skeleton Stress-Strain Curve

The skeleton stress-strain curve is that part of the stress-strain characteristic that is history-independent; it is therefore geometrically similar to the invariant nonlinear portion of the hysteresis curve, but reduced by a factor of two. A convenient method of determining the history-independent portion of the hysteresis curve is to translate the hysteresis loops plotted in Figure 5 along the elastic slope until their upper branches are matched as well as possible (Figure 6). The portion OAB of the hysteresis curve in Figure 6, when reduced by a factor of two, will define the skeleton stress-strain curve. The cyclic stress-strain curve and the skeleton stress-strain curve can also be expressed as stress-plastic strain relationships by eliminating elastic strain components from total strains.

Saturation Yield Strength Increment

The saturation Yield Strength Increment (YSI), which is one-half of YRI, is usually expressed as a function of stress, strain, or plastic strain amplitude. It is given by the difference in stress level between the cyclic stress-strain curve (Figure 7) and the skeleton stress-strain curve expressed as a function of plastic strain. As the name denotes, it represents the change in the material's yield strength as a function of loop size.

[27]R. W. Landgraf, J. Morrow, and T. Endo, "Determination of the Cyclic Stress-Strain Curve," *ASTM Journal of Materials*, JMLSA, Vol 4, No. 1 (American Society for Testing and Materials, March 1969), pp 176-188.

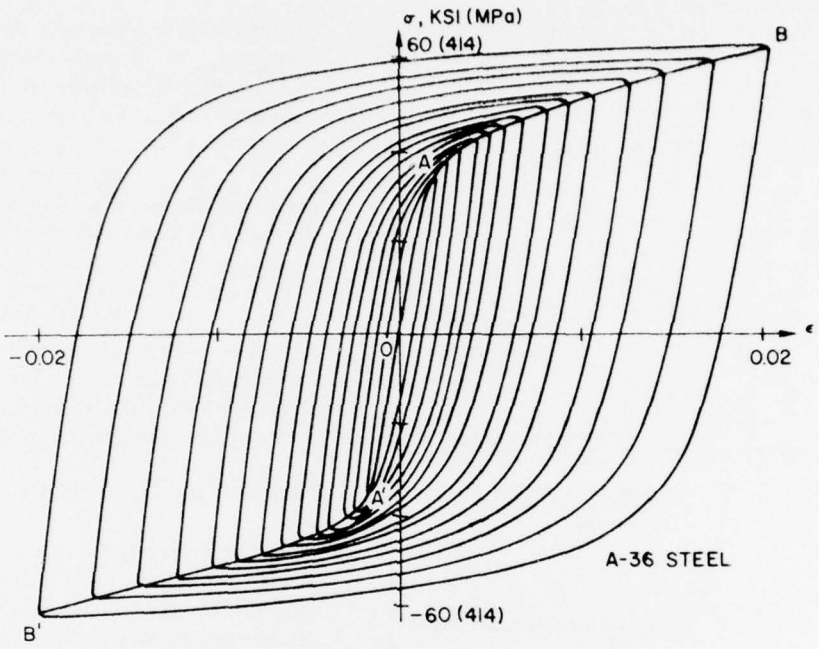

Figure 4. Stable hysteresis loops with cyclic stress-strain curve (B'A'OAB).

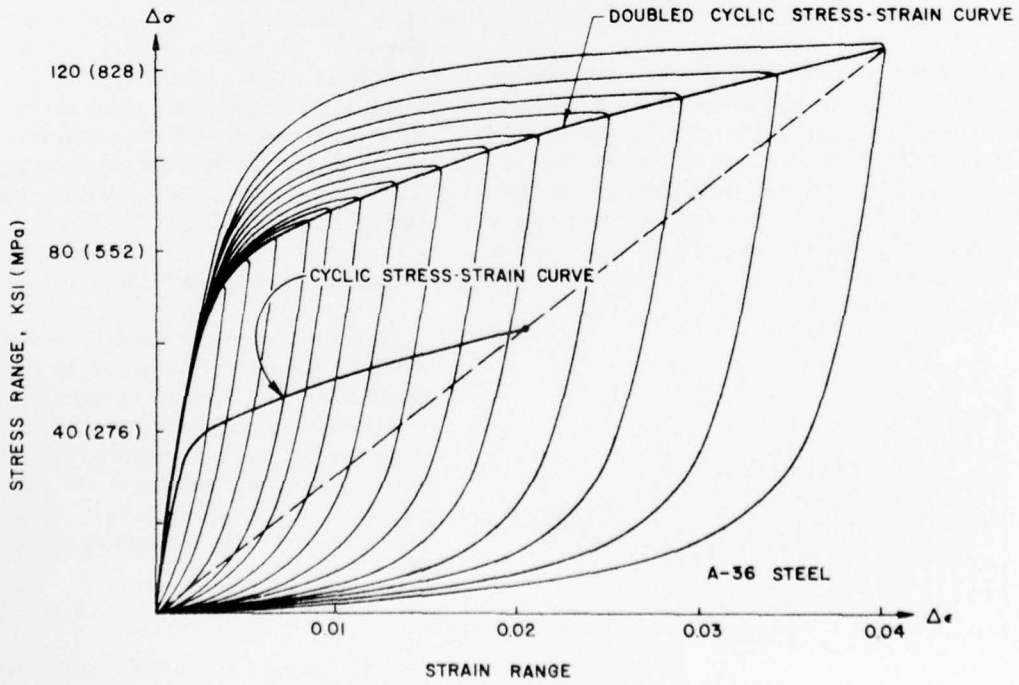

Figure 5. Stable hysteresis loops (of Figure 4) superimposed on their lower tips.

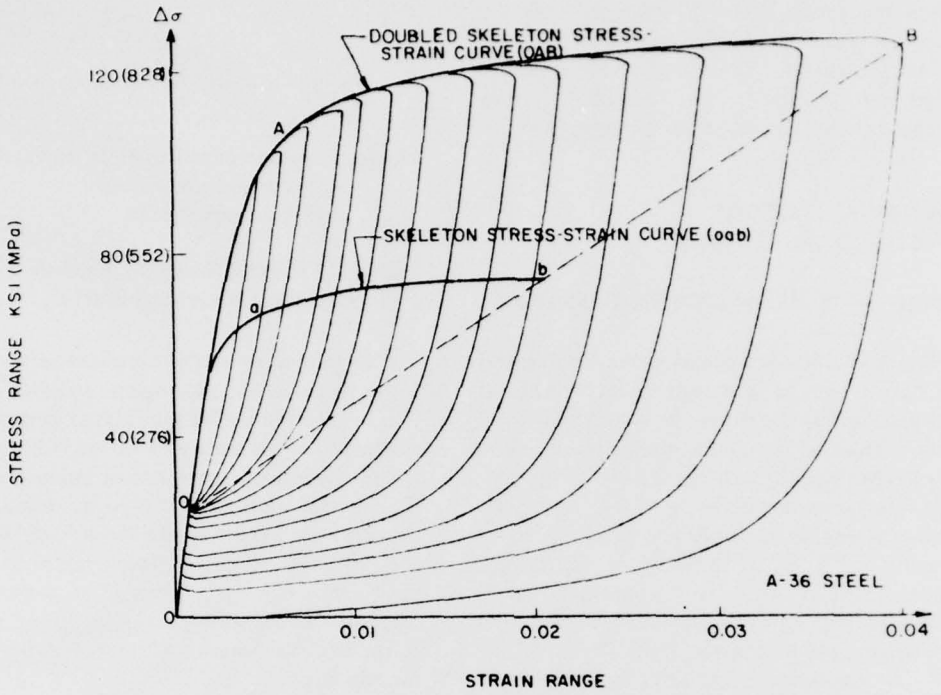

Figure 6. Stable hysteresis loops (of Figure 5) translated along the elastic slopes.

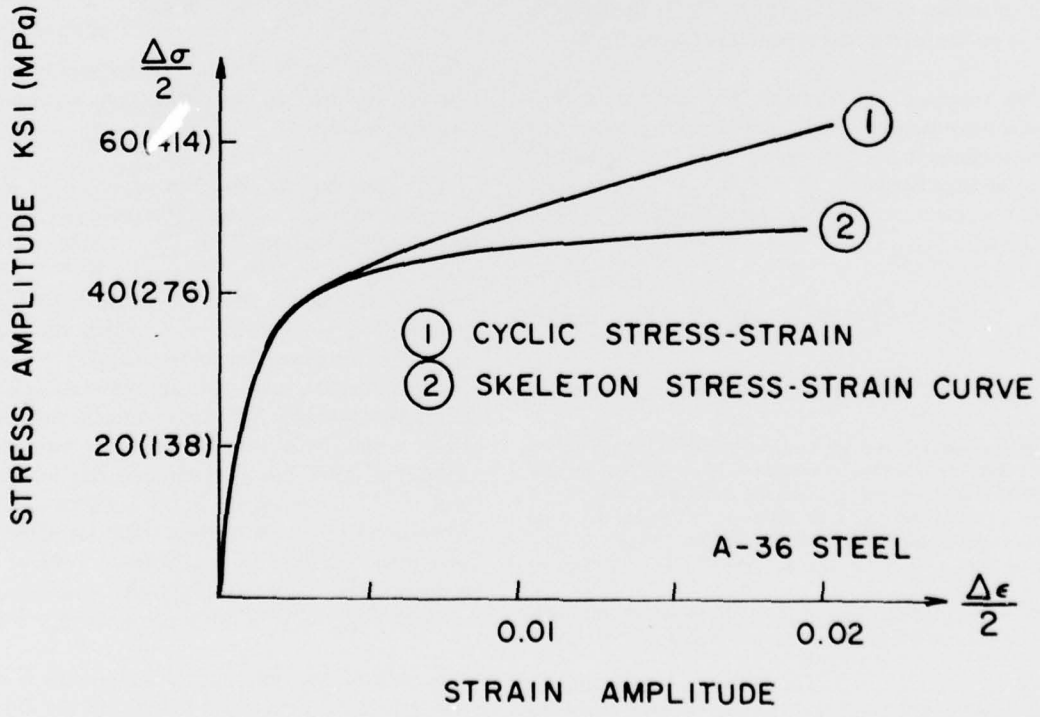

Figure 7. Comparison between cyclic and skeleton stress-strain curves of A-36 steel.

If the saturation YSI or YRI is independent of the hysteresis loop size, as in the case of 2024-T4 aluminum, then the cyclic stress-strain curve and the skeleton stress-strain curve differ only in their elastic portions by a constant value. These materials are designated as "Masing" type materials, since Masing's postulation implies such a property.[28]

4 MULTIAXIAL THEORY OF CYCLIC PLASTICITY

Generalization of Uniaxial Cyclic Properties

The previously discussed observations for uniaxial cyclic behavior can be generalized for multiaxial stress space following the theory proposed by Mroz[29] and Iwan.[30] The skeleton stress-plastic strain curve OS shown schematically in Figure 8(a) is approximated by N linear segments OA, AB, BC, . . ., MN. Nodal stress values corresponding to points A, B, C, . . ., N are $\bar{\sigma}^{(0)}$, $\bar{\sigma}^{(1)}$, $\bar{\sigma}^{(2)}$, . . ., $\bar{\sigma}^{(N-1)}$, respectively. In a general stress space, this approximation is represented by nesting hypersurfaces $f^{(0)}$, $f^{(1)}$, $f^{(2)}$, . . ., $f^{(N)}$ (Figure 8b) with initial radii $\bar{\sigma}^{(0)}$, $\bar{\sigma}^{(1)}$, $\bar{\sigma}^{(2)}$, . . ., $\bar{\sigma}^{(N-1)}$, respectively. Initially, these hypersurfaces are concentric, with their centers at a point 0 representing zero stress level in the stress space. The first (smallest) of these surfaces, $f^{(0)}$, is the conventional yield surface and represents elastic limit.

The hypersurfaces translate and expand or contract during plastic flow. Instantaneous positions of these surfaces in the stress space are given by coordinates of their origins, $a_{ij}^{(n)}$, n = 0, 1, . . ., (N − 1). The hypersurfaces can be mathematically represented as

$$f^{(n)} = \frac{1}{2} p_{ij}^{(n)} p_{ij}^{(n)} - \frac{1}{3}(\bar{\sigma}^{(n)})^2 = 0 \qquad \text{[Eq 1]}$$

(summation is implied)

in which n = 0, 1, 2, . . ., N − 1, where a von Mises yield condition (given by $f^{(0)} = 0$ for plastic flow) is used, and

$$p_{ij}^{(n)} = \sigma_{ij} - a_{ij}^{(n)} - \frac{1}{3}\delta_{ij}(\sigma_{kk} - a_{kk}^{(n)}) \qquad \text{[Eq 2]}$$

where $\bar{\sigma}^{(i)}$ = current radius of the surface $f^{(i)}$
σ_{ij} = current stress state
δ_{ij} = Kronecker delta.

Fields of Plastic Tangent Moduli and Isotropic Hardening Moduli

A slope at any point of the skeleton curve of Figure 8a is defined as plastic tangent modulus. This definition of plastic tangent modulus is generalized for a multiaxial stress state as follows. It is assumed that the projection of increment of stress vector $d\sigma_{ij}$ on the exterior normal to the yield surface is proportional to the plastic strain vector $d\varepsilon_{ij}^{p}$. Therefore, if the projection of $d\sigma_{ij}$ on the exterior normal to the yield surface is $cd\varepsilon_{ij}^{p}$, where c is a proportionality constant, then a vector $(d\sigma_{ij} - cd\varepsilon_{ij}^{p})$ is perpendicular to the exterior normal. Mathematically, this can be expressed as

$$(d\sigma_{ij} - cd\varepsilon_{ij}^{p})\frac{\partial f^{(0)}}{\partial \sigma_{ij}} = 0 \qquad \text{[Eq 3]}$$

where $\partial f^{(0)}/\partial \sigma_{ij}$ is the exterior normal to the yield surface, and the proportionality constant c is plastic tangent modulus.

In Figure 8a, the skeleton curve of the uniaxial case has been approximated by piecewise linear segments. Nodal points 0, 1, 2, . . ., (N − 1) are at stress levels $\bar{\sigma}^{(0)}$, $\bar{\sigma}^{(1)}$, $\bar{\sigma}^{(2)}$, . . ., $\bar{\sigma}^{(N-1)}$, respectively. Each nodal point m is associated with a plastic tangent modulus $c^{(m)}$, which remains constant between the nodal points m and m + 1. For the multiaxial stress state, this approximation is generalized by assuming that plastic tangent modulus c of Eq 3 remains constant between any two surfaces. This constant value of c between the surfaces $f^{(m)}$ and $f^{(m+1)}$ is given by $2c^{(m)}/3$ where $c^{(m)}$ is the corresponding plastic tangent modulus of the piecewise linear skeleton curve. Thus, a field of plastic tangent moduli is constituted by associating a plastic tangent modulus $c^{(m)}$ to the hypersurface $f^{(m)}$.

A field of isotropic hardening moduli is defined similarly as the field of plastic tangent moduli. In the uniaxial case, stress levels $\bar{\sigma}^{(i)}$ associated with the

[28] H. R. Jhansale, "A Friction Stress Method for the Cyclic Inelastic Behavior of Metals," *Transactions of the 3rd International Conference on Structural Mechanics in Reactor Technology*, Vol 5, Paper L5/4 (1975); and H. R. Jhansale, "A New Parameter for the Hysteretic Stress-Strain Behavior of Metals," *Journal of Engineering Materials and Technology*, Vol 97, No. 1 (1975), pp 33-38.

[29] Z. Mroz, "On the Description of Anisotropic Workhardening," *Journal of Mechanics of Physical Solids*, Vol 15 (1967), pp 163-175.

[30] W. D. Iwan, "On a Class of Models for the Yielding Behavior of Continuous and Composite Systems," *Journal of Applied Mechanics*, Vol 34 (1967), pp 612-617.

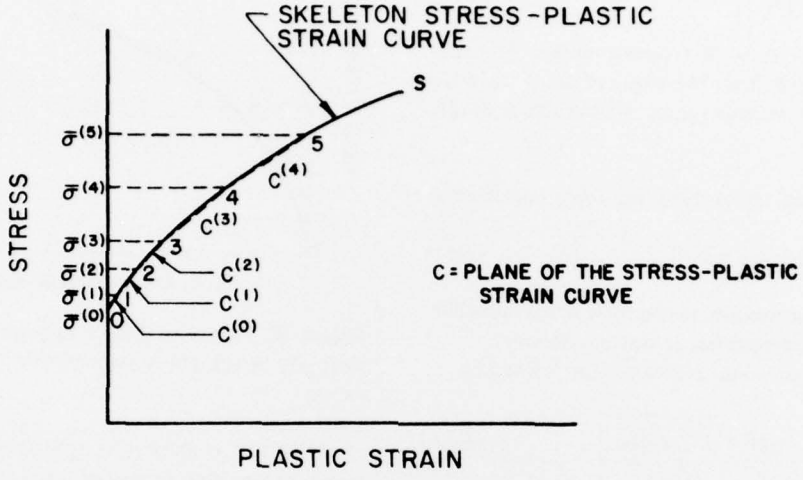

(a) Skeleton stress-plastic strain curve.

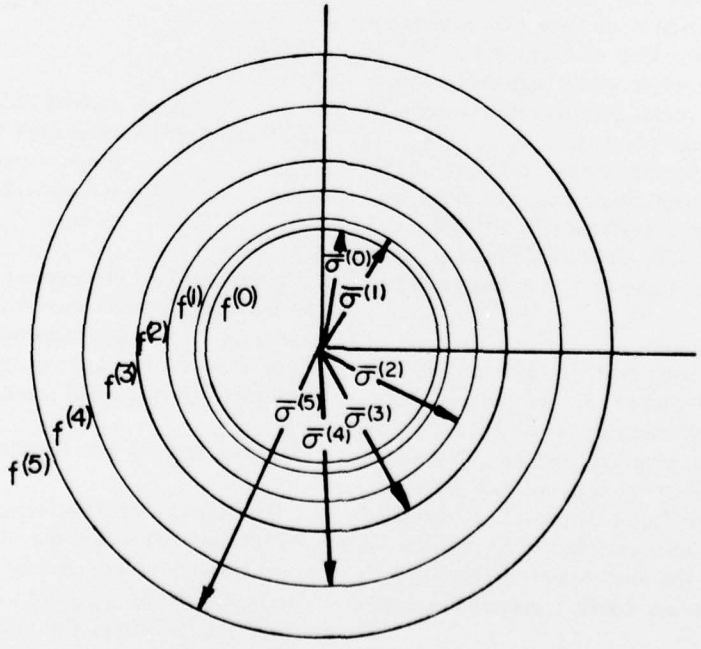

(b) Hypersurfaces in stress space.

Figure 8. Schematic representation of hypersurfaces.

piecewise approximation of the skeleton curve, are given increments of $d\bar{\sigma}^{(i)}$ to reflect isotropic hardening. All these increments are assumed to be the same to insure the history-independent nature of the skeleton curve. These increments are assumed to be proportional to the increment of plastic strain.

$$d\bar{\sigma}^{(i)} = k d\bar{\varepsilon}^{p},\ i = 0, 1, 2, \ldots, (N-1) \quad [Eq\ 4]$$

where k is the constant of proportionality. The constant k is obtained from the slope of the saturation yield strength increment versus plastic strain amplitude curve.

For a multiaxial stress state, Eq 4 is generalized as

$$d\bar{\sigma}^{(i)} = h d\bar{\varepsilon}^{p},\ i = 0, 1, 2, \ldots, (N-1) \quad [Eq\ 5]$$

where $d\bar{\sigma}^{(i)}$ = increments in the radii of surfaces $f^{(i)}$
h = isotropic hardening coefficient
$d\bar{\varepsilon}^{p}$ = equivalent plastic strain defined by

$$d\bar{\varepsilon}^{p} = \sqrt{\frac{2}{3} d\varepsilon_{ij}^{p} d\varepsilon_{ij}^{p}} \quad [Eq\ 6]$$

where $d\varepsilon_{ij}^{p}$ is increment of plastic strain.

The isotropic hardening coefficient h is assumed to be constant between any two hypersurfaces $f^{(m)}$ and $f^{(m+1)}$ and is given by a value $h^{(m)}$ associated with the surface $f^{(m)}$. This constant value $h^{(m)}$ is obtained from a piecewise linear approximation of the saturation YSI versus plastic strain amplitude curve (Figure 9). Nodal points 0, 1, 2, . . ., (N − 1) on this curve are at the same stress levels as the nodal points of the piecewise linear skeleton curve and therefore correspond to surfaces $f^{(0)}$, $f^{(1)}$, $f^{(2)}$, . . ., $f^{(N-1)}$, respectively. The slope of a linear segment between nodal points i and (i + 1) is designated as $k^{(i)}$.

The first time a stress path extends into the zone between surfaces $f^{(i)}$ and $f^{(i+1)}$, the isotropic hardening modulus $h^{(i)}$ corresponding to the surface $f^{(i)}$ is given by $k^{(i)}$. For any subsequent stress excursion into this zone, $h^{(i)}$ is set equal to one-half of $k^{(i)}$, except when i = 0. This factor of one-half is necessary to properly reflect the scale factor of two that is associated between the monotonic and cyclic paths in the uniaxial case (see **Cyclic Uniaxial Properties** section in Chapter 3).

For subsequent stress excursions into the zone between surfaces $f^{(0)}$ and $f^{(1)}$, the isotropic hardening

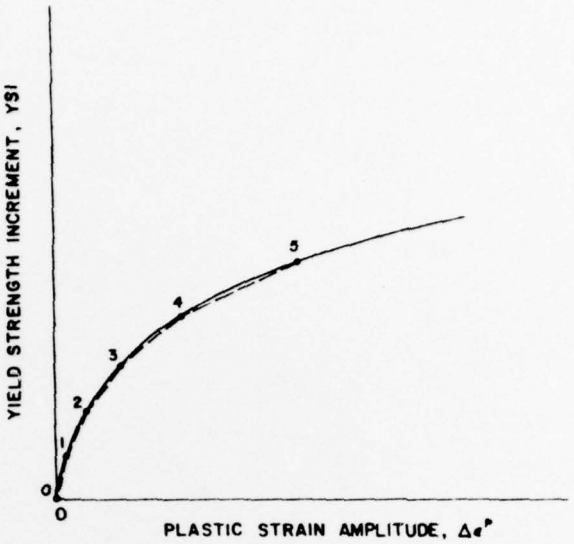

Figure 9. Piecewise linear approximation of yield strength increment versus plastic strain amplitude curve.

modulus $h^{(0)}$ is chosen to approximately reflect the non-Masing and transient characteristics of real materials in the uniaxial case:

$$h^{(0)} = -f \frac{[\delta\sigma_y - \delta\sigma_y^{(1)}]}{\Delta\varepsilon^{p(1)}} \quad [Eq\ 7]$$

where

$\delta\sigma_y$ = current YSI
$\delta\sigma^{(1)}$ and $\Delta\varepsilon^{p(1)}$ = saturation YSI and plastic strain range corresponding to node 1
f = softening/hardening factor $\simeq$ 0.8 to 1.

The value of f = 1 eliminates transient behavior (i.e., a gradual approach toward saturation); f < 1 provides for the transient behavior, but the exact saturation value of YSI is not reached. A value of f = 0.8 to 0.9 seems to be a good compromise.

Translations of the Hypersurfaces

Translations of these hypersurfaces are governed by the conditions that the surfaces do not intersect but consecutively contact and push each other. They may contact only at a point which corresponds to the current stress state. For convex and geometrically similar surfaces, these conditions may be satisfied by requiring that instantaneous motions of the surfaces be in a specific direction. This direction is along a

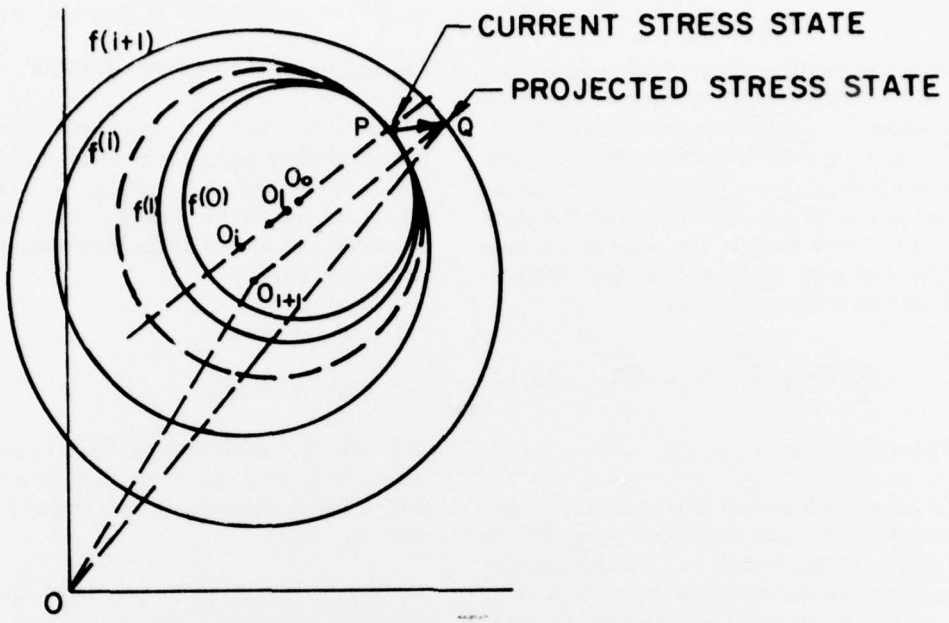

Figure 10. Schematic translations of hypersurfaces in stress space.

vector connecting the point of contact (current stress state) with a point on the next surface to be encountered, which has a same normal direction as the normal to the yield surface at the point of contact.

Translation vectors $a_{ij}^{(m)}$, m = 0, 1, . . ., (N − 1) can now be obtained by considering the example given in Figure 10. Surfaces $f^{(0)}$, $f^{(1)}$, . . ., $f^{(i)}$ are in contact at a point P corresponding to the current stress state σ_{ij}. Current origins of these surfaces are denoted by 0_0, 0_1, . . ., 0_i. The next surface to be encountered is $f^{(i+1)}$ with origin at 0_{i+1}. Instantaneous motions of all the surfaces will be along the vector PQ, where Q is a point having the same normal to $f^{(i+1)}$ as the normal to the yield surface at P. Stress state at Q is designated as projected stress state. Its coordinates are denoted by σ_{ij}^{q}.

To obtain coordinates σ_{ij}^{q}, a vector $\overrightarrow{0_{i+1}Q}$ is drawn parallel to $\overrightarrow{0_0P}$. Homogeneity of Eq 1 yields

$$\overrightarrow{0_{i+1}Q} = \frac{\bar{\sigma}^{(i+1)}}{\bar{\sigma}^{(0)}}\overrightarrow{0_0P} \qquad \text{[Eq 8]}$$

where $\bar{\sigma}^{(0)}$ = current radius of the yield surface and
$\bar{\sigma}^{(i+1)}$ = current radius of the surface $f^{(i+1)}$.

Therefore,

$$\overrightarrow{0_{i+1}Q} = \frac{\bar{\sigma}^{(i+1)}}{\bar{\sigma}^{(0)}}(\sigma_{ij} - a_{ij}^{(0)}) \qquad \text{[Eq 9]}$$

Coordinates of point Q are given by

$$\sigma_{ij}^{q} = \overrightarrow{00}_{i+1} + \overrightarrow{0_{i+1}Q} \qquad \text{[Eq 10]}$$

Substituting for $0_{i+1}Q$ from Eq 9,

$$\sigma_{ij}^{q} = a_{ij}^{(i+1)} + \frac{\bar{\sigma}^{(i+1)}}{\bar{\sigma}^{(0)}}(\sigma_{ij} - a_{ij}^{(0)})$$

Instantaneous motion of the yield surface can now be written as

$$da_{ij}^{(0)} = d\mu\,(\sigma_{ij}^{q} - \sigma_{ij}) \qquad \text{[Eq 11]}$$

where $da_{ij}^{(0)}$ is an increment of the translation vector of yield surface and $d\mu$ is a scalar parameter. Eq 11 was first introduced by Mroz[31] and is often referred to as Mroz's kinematic hardening law.

The parameter $d\mu$ is obtained by satisfying the condition that the current stress state remains on the yield surface. Appendix A provides the derivation of

[31] Z. Mroz, "On the Description of Anisotropic Workhardening," *Journal of Mechanics of Physical Solids*, Vol 15 (1967), pp 163-175.

an expression for $d\mu$ in terms of stresses and stress increments.

Coordinates of the new origin of the yield surface are obtained by adding $da_{ij}^{(0)}$ to the coordinates of previous origin. Coordinates of new origins of the remaining surfaces in contact at $P(f^{(1)}, f^{(2)}, \ldots, f^{(i)})$ are determined by requiring that these surfaces remain in contact at the new stress state and that their origins remain on a straight line joining the new stress state and new origin of the yield surface. Hence, it can be easily shown that

$$a_{ij}^{(m)} = \sigma_{ij} - \frac{\bar{\sigma}^{(m)}}{\bar{\sigma}^{(0)}}(\sigma_{ij} - a_{ij}^{(0)}), \qquad \text{[Eq 12]}$$

in which $m = 1, 2, \ldots, i$.

The surfaces which are not in contact at the current stress state are also translated along PQ to retain the shape of the skeleton curve under uniaxial cyclic loading. Any increments in the radii of these surfaces tend to distort the skeleton curve. To offset this effect, origins of these surfaces are translated so that measures of their translations are equal and opposite to the increments in their radii. Therefore,

$$da_{ij}^{(m)} = d\gamma\eta_{ij}, m = i+1, i+2, \ldots, N-1 \qquad \text{[Eq 13]}$$

where $d\gamma$ is the measure (magnitude) of $da_{ij}^{(\eta)}$:

$$d\gamma = -h^{(i)}d\bar{\varepsilon}^{p}, \qquad \text{[Eq 14]}$$

and η_{ij} is a unit vector along $\overrightarrow{PQ}$:

$$\eta_{ij} = \frac{(\sigma_{ij}^{q} - \sigma_{ij})}{[(\sigma_{mn}^{q} - \sigma_{mn})(\sigma_{mn}^{q} - \sigma_{mn})]^{1/2}}$$

Eqs 5, 11, 12, and 13 completely specify expansions (or contractions) and translations of these surfaces. The plasticity formulation can now be completed with the following flow rule[32]:

$$d\varepsilon_{ij}^{p} = d\lambda \frac{\partial f^{(0)}}{\partial \sigma_{ij}} \qquad \text{[Eq 15]}$$

where $d\lambda$ is a scalar parameter given by

$$d\lambda = \frac{P_{ij}^{(0)} d\sigma_{ij}}{(2c/3)(\bar{\sigma}^{(0)})^2} \qquad \text{[Eq 16]}$$

[32]R. Hill, *The Mathematical Theory of Plasticity* (Oxford, 1950).

Appendix B provides the derivation of Eq 15 and the other equations used in the plastic analysis.

Algorithm for Numerical Analysis

This section gives an algorithm for calculating a new stress state $(\sigma_{ij})_{new}$ at the end of a given strain increment $d\varepsilon_{ij}$ by the plasticity formulation presented in this report. The following variables are assumed to be known at the beginning of the given strain increment:

1. Current strain ε_{ij}

2. Current stress σ_{ij}

3. ISURF = number of the largest surface in contact at the current stress state. (If the current stress state is within the yield surface, then ISURF is set equal to −1.)

It is assumed that strain increments $d\varepsilon_{ij}$ are small enough that changes in the plastic tangent modulus and the isotropic hardening modulus are small. If $d\varepsilon_{ij}$ are not small, then they are subdivided into smaller increments before the following algorithm is applied.

Step 1. Define new variables τ_{ij} and de_{ij} by

$$\tau_{ij} = \sigma_{ij},$$
$$de_{ij} = d\varepsilon_{ij}$$

Assuming an elastic behavior, calculate $d\tau_{ij}$ from strain increment de_{ij}, using Eq B7 of Appendix B.

Step 2. Calculate a trial stress state T :

$$T_{ij} = \tau_{ij} + d\tau_{ij}.$$

Step 3. a. If the yield function $f^{(0)} = f^{(0)}(T_{ij}, a_{ij}^{(0)}, \bar{\sigma}^{(0)}) \leqslant 0$, then the assumption of elastic behavior is valid. Therefore, the new stress state is given by

$$(\sigma_{ij})_{new} = T_{ij}.$$

ISURF is updated by setting it equal to −1. This completes calculations for the current strain increment.

b. If $f^{(0)} > 0$ and ISURF = −1, then transition from elastic to plastic behavior takes place. Go to Step 6.

c. If $f^{(0)} > 0$ and ISURF ≥ 0, then plastic loading continues. Go to Step 4.

Step 4. From the strain increment de_{ij}, determine stress increment $d\tau_{ij}$, using Eq B11. Material constant c in this equation is given by the plastic tangent modulus $c^{(n)}$, where n = ISURF. Calculate a new trial state T_{ij} by

$$T_{ij} = \tau_{ij} + d\tau_{ij},$$

and go to Step 5.

Step 5. Determine $f^{(n)}(T_{ij}, a_{ij}^{(n)}, \bar{\sigma}^{(n)})$, n = ISURF + 1.

a. If $f^{(n)} \leq 0$, then the stress state remains within the surface $f^{(n)}$, n = ISURF + 1. Therefore, the trial stress state is the new stress state, as shown by

$$(\sigma_{ij})_{new} = T_{ij}.$$

Updating the radii and origins of the hypersurfaces (see Chapter 4) will complete calculations for the current strain increment.

b. If $f^{(n)} > 0$, go to Step 6.

Step 6. Determine a variable RATIØ such that

$$f^{(n)}(\tau_{ij} + \text{RATIØ} * d\tau_{ij}, a_{ij}^{(n)}, \bar{\sigma}^{(n)}) = 0,$$

where n = ISURF + 1.

Redefine τ_{ij} as the stress on $f^{(n)}$, n = ISURF + 1.

$$\tau_{ij} = \tau_{ij} + \text{RATIØ} * d\tau_{ij}$$

Redefine strain increment:

$$de_{ij} = (1 - \text{RATIØ}) * de_{ij}$$

Update radii and origins of the surfaces (see Chapter 4). Update ISURF by increasing it by one and go back to Step 4.

5 DISCUSSION

There are two major differences between the present formulation and most others in the literature. First, the present approach uses a skeleton curve derived from uniaxial cyclic tests instead of a uniaxial monotonic stress-strain curve. The second major difference is that the yield strength in other formulations is assumed to be a function of a monotonically increasing parameter. This restricts the material to harden or soften monotonically, regardless of the nature of cyclic loading. Therefore, in contrast to the present formulation (where yield strength increments are defined from a field of isotropic hardening moduli), other formulations cannot exhibit transient hardening or softening.

The plasticity formulation developed in this report is capable of closely simulating all the important cyclic material characteristics* under the uniaxial stress state. However, to demonstrate the real worth of the present approach, its predictive capabilities must be verified under multiaxial stress states. Although a few multiaxial cyclic stress-strain data are available in the literature, attendant cyclic uniaxial properties for the same material have not been generated or reported. Since the present formulation requires cyclic uniaxial material properties as a base, its predictive capabilities cannot be tested for such data. A limited experimental program to test the present formulation under a biaxial stress state is in progress.

However, significant differences between the present approach and alternative approaches currently in use for general structural analysis (isotropic hardening and kinematic hardening) can be effectively demonstrated for a typical uniaxial cyclic material behavior. The simplest and most important feature in a uniaxial cyclic response is the saturated hysteresis loop under constant strain limit cycles, because the material rapidly approaches this state and remains there for a major portion of its cyclic (fatigue) life. Therefore, the accuracy with which this saturation hysteresis loop is predicted gives a reasonable measure of the adequacy of a plasticity formulation.

Figures 11, 12, 13, and 14 show hysteresis loops predicted by different methods for two materials—A-36 steel (hot worked) and SAE 1005-1009 steel (cold rolled). Real hysteresis loops of these steels (not shown in the figures) are nearly identical to those predicted by the present plasticity formulation. If the plastic tangent modulus of a material is nonzero for large values of plastic strain, then isotropic hardening will predict continuously growing (or contracting, if the modulus is negative) hysteresis loops.

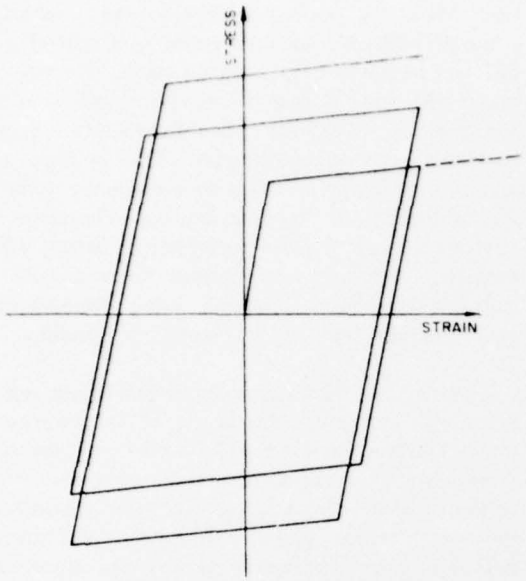

Figure 11. Bilinear hysteresis loops predicted by isotropic hardening theory for A-36 steel.

Figure 11 shows such hysteresis loops for A-36 steel. If the plastic tangent modulus approaches zero for large plastic strains, then hysteresis loops predicted by the isotropic hardening theory will stabilize after a sufficient number of cycles. This is illustrated in Figure 12 for SAE 1005-1009 steel. However, once these loops are stabilized, the isotropic hardening theory reduces to a perfect plasticity theory which does not allow any change in the yield range of the material. In the case of the kinematic hardening theory, yield ranges of all stabilized hysteresis loops remain the same (twice the yield strength) and slopes of their elasto-plastic branches are equal to the slope of the uniaxial stress-strain curve at a large value of plastic strain. Figures 13 and 14 compare the stabilized hysteresis loops predicted by the kinematic hardening theory and the present plasticity formulation. These figures clearly show that stress-strain responses and energy absorption estimates (determined from areas enclosed by the hysteresis loops) can be significantly erroneous if not represented accurately. This error becomes more critical if the material is subjected to irregular or variable load histories.

6 APPLICATION TO SEISMIC DESIGN PROCEDURES

The plasticity formulation described in this report can be used advantageously in several areas of seismic design. For example, consider the typical seismic design procedure outlined by Newmark and Hall[33] and shown in Figure 15. The procedure has five steps. First, an earthquake hazards or seismic risk is selected for a site based on the geographic location of the structure, its vicinity from active faults, soil conditions at the site, and past earthquake activity in that region. Second, a safety factor, allowable deformation limit, and allowable probability of damage are selected. These selections are influenced by the functional requirements of the structure and the costs of a failure in terms of human lives, disrupted services, labor, and materials. The values selected in this step may also depend on the type and layout of the structure as determined in step 3. Preliminary design, step 3, is accomplished in accordance with design codes and past experience. Approximate estimates of the structure's static and dynamic strengths, ductility, and natural frequency, damping, and energy absorption characteristics are also made. In step 4 the overall adequacy of the structure is verified and the strength or other parameters are changed as necessary. Steps 3 and 4 are repeated until a satisfactory design of the structure is achieved. At this point the design is considered final for many types of structures for which a large safety factor is implicit in the design criteria. In such cases step 5 is not undertaken. However, it is important that the design of critical facilities such as hospitals, schools and nuclear containment vessels be verified by an analysis (step 5) in which structural characteristics (strength, damping, energy dissipation, etc.) are estimated more accurately by advanced structural techniques. Such an analysis may indicate need for further changes in the design and a requirement to repeat steps 3, 4, and 5.

Energy dissipation characteristics of a structure are estimated (approximately in step 3 and more accurately in step 5) to ensure that the structure can absorb the energy imparted to it by ground motion, blast forces, or strong winds. An inability to absorb this energy without excessive deformations or a long transient response may result in catastrophic failure. Energy dissipation is usually roughly estimated by assigning some damping coefficients to the structure. These coefficients are chosen on the basis of past experience and can be verified only by accurately determining the deformation response and associated energy dissipation of several typical structures. Therefore, the research conducted under this

[33] N. M. Newmark and W. J. Hall, "Procedures and Criteria for Earthquake Resistant Design," *Building Practices for Disaster Mitigation*, BSS-46 (National Bureau of Standards, 1973).

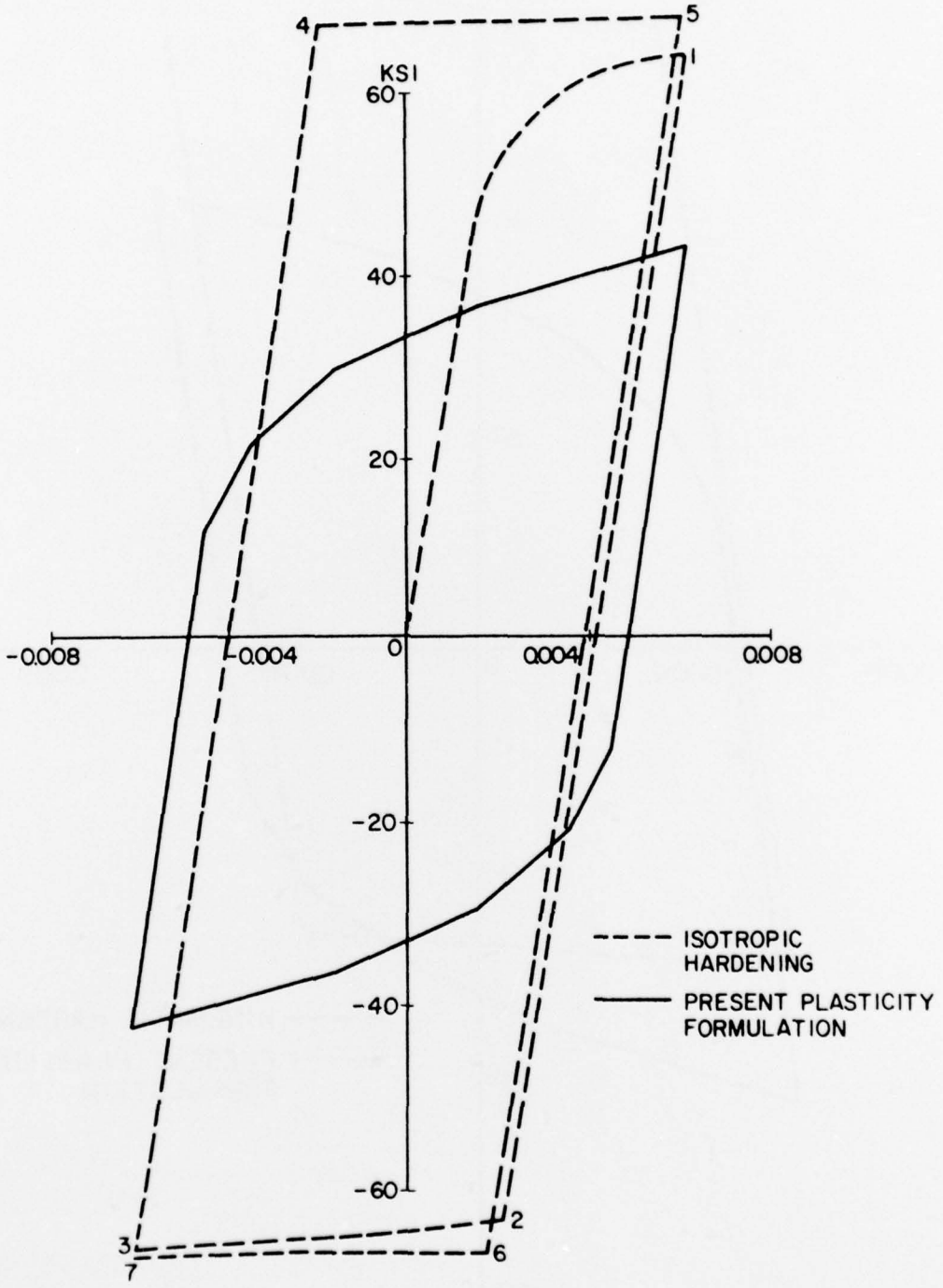

Figure 12. Hysteresis loops of SAE 1005-1009 steel (cold rolled).

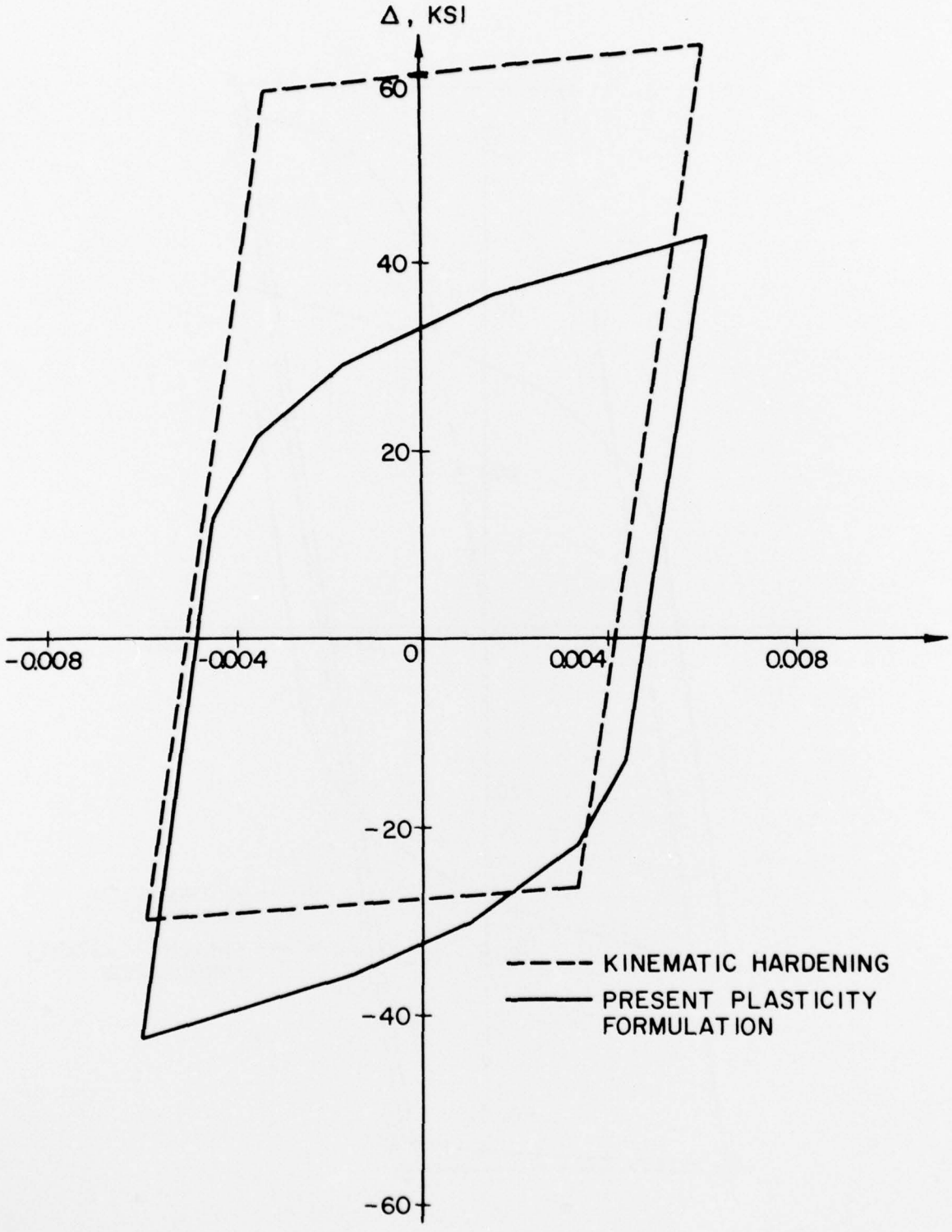

Figure 13. Stabilized hysteresis loops of SAE 1005-1009 steel (cold rolled).

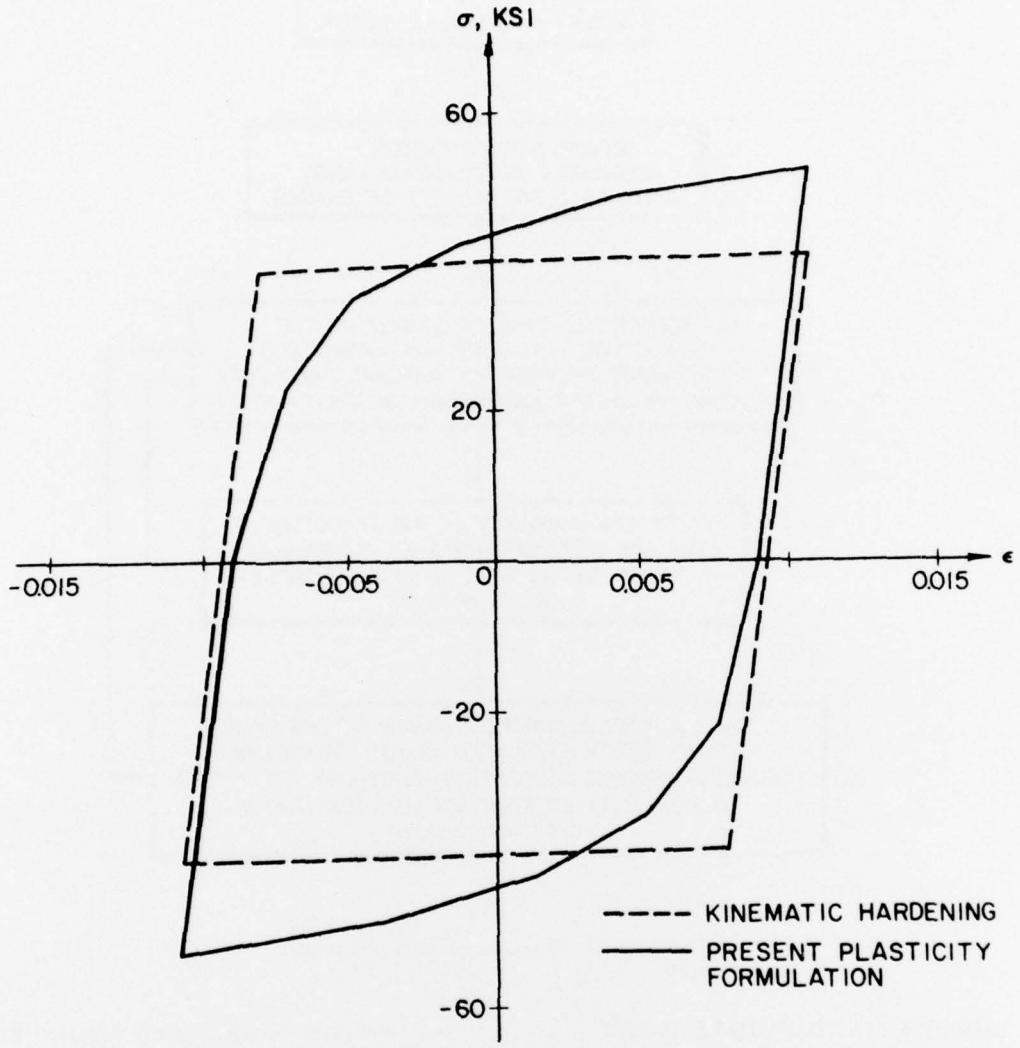

Figure 14. Stabilized hysteresis loops of A-36 steel (hot worked).

project has an impact on seismic design procedures in the following areas:

1. Results of accurate inelastic analyses (step 5) will provide guidelines for developing structural strength criteria (step 3) under inelastic loading conditions.

2. Energy dissipation caused by cyclic inelastic deformations will provide a rational basis for determining damping coefficients at high stress levels (to be used in step 3).

3. Conservative and elastic designs will be replaced by inelastic designs, resulting in substantial savings in labor and materials costs.

4. Cyclic inelastic analyses will accurately determine the deformation response and safety of existing critical structures (step 5).

5. The capability to perform an accurate structural analysis will enable designers to use novel design concepts with confidence. This will allow more creativity in the use of space and materials.

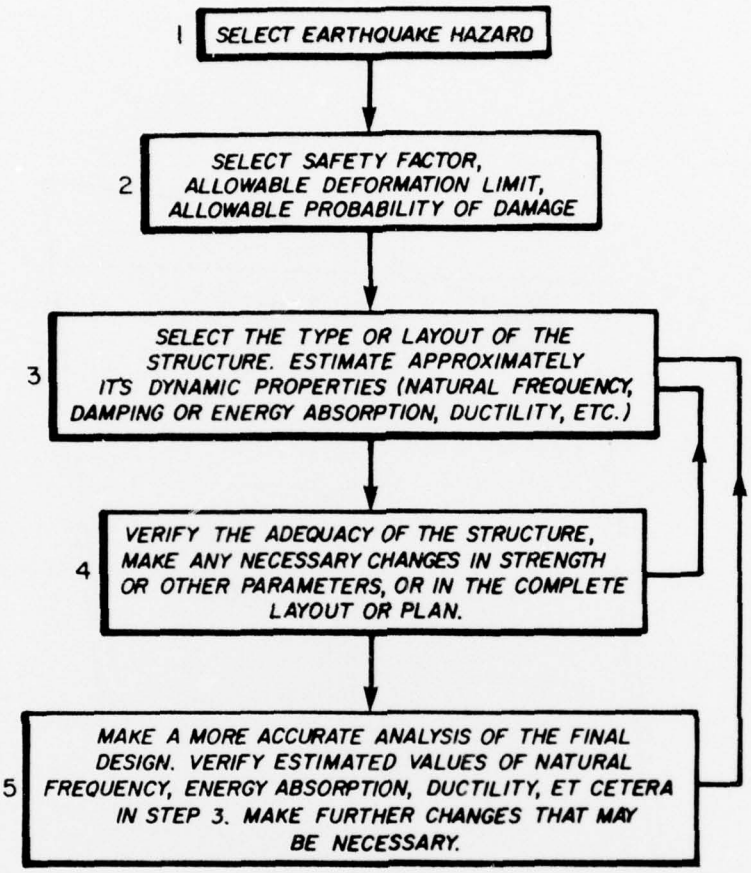

Figure 15. A seismic design procedure.

7 SUMMARY AND FUTURE WORK

Summary

This report has presented a plasticity formulation adequate for cyclic inelastic structural analysis; appropriate cyclic material properties required by this formulation can be determined from simple cyclic uniaxial tests. This formulation is capable of simulating all the important cyclic material phenomena of deformation response, including memory of prior history and non-Masing type of behavior. The need for classifying a general loading path into a plastic loading or a plastic load reversal cyclic analysis has been eliminated. Hysteresis loops predicted by the present formulation are very close to a material's actual hysteresis loops. These loops have been shown to be significantly different from those predicted by other plasticity theories currently used in finite element codes. Therefore, using the present formulation in existing nonlinear programs will achieve a reliable and accurate estimation of energy dissipation and deformation response.

Future Work

Future research for this project includes (1) experimental verification of the plasticity formulation presented in this report under a cyclic tension-torsion state, and (2) an analysis of multiaxial inelastic hysteretic behavior of reinforced concrete structural members. The results obtained in this project will be translated into simplified design procedures to be incorporated into the *Seismic Design of Buildings*, TM5-809-10 series.

REFERENCES

Dafalias, Y. F. and E. P. Popov, "A Model of Nonlinearly Hardening Materials for Complex Loading," *Acta Mechanica*, Vol 21 (1975), pp 173-192.

Eisenberg, M. A., "A Generalization of Plastic Flow Theory With Application to Cyclic Hardening and Softening Phenomena," *Journal of Engineering Materials and Technology*, Vol 98, Series H, No. 3 (July 1976), pp 221-228.

Felter, C. E. and C. Laird, "Cyclic Stress-Strain Response of FCC Metals and Alloys," *ACTA Metallurgica*, Vol 15 (October 1967).

Hill, R., *The Mathematical Theory of Plasticity* (Oxford, 1950).

Iwan, W. D., "On a Class of Models for the Yielding Behavior of Continuous and Composite Systems," *Journal of Applied Mechanics*, Vol 34 (1967), pp 612-617.

Jhansale, H. R., "A Friction Stress Method for the Cyclic Inelastic Behavior of Metals," *Transactions of the 3rd International Conference on Structural Mechanics in Reactor Technology*, Vol 5, Paper L5/4 (1975).

Jhansale, H. R., "A New Parameter for the Hysteretic Stress-Strain Behavior of Metals," *Journal of Engineering Materials and Technology*, Vol 97, No. 1 (1975), pp 33-38.

Jhansale, H. R. and T. H. Topper, "An Engineering Analysis of the Inelastic Stress Response of a Structural Metal Under Variable Cyclic Strain," *Experimentation and Failure Prediction*, STP-519 (American Society for Testing and Materials, 1973).

Krieg, R. D., "A Practical Two Surface Plasticity Theory," *Journal of Applied Mechanics*, Vol 42 (1975), pp 641-646.

Landgraf, R. W., J. Morrow, and T. Endo, "Determination of the Cyclic Stress-Strain Curve," *ASTM Journal of Materials*, JMSLA, Vol 4, No. 1 (American Society for Testing and Materials, March 1969), pp 176-188.

McNamara, J. F. and S. K. Sharma, *Isotropic-Kinematic Hardening Model for Elastic-Plastic Structural Analysis*, Technical Report M-148/ADA014945 (Construction Engineering Research Laboratory [CERL], August 1975).

Mroz, Z., "An Attempt to Describe the Behavior of Metals Under Cyclic Loads Using a More General Workhardening Model," *Acta Mechanica*, Vol 7, No. 2-3 (1969), pp 199-212.

Mroz, Z., "On the Description of Anisotropic Workhardening," *Journal of Mechanics of Physical Solids*, Vol 15 (1967), pp 163-175.

Mura, T., "Continuum Theory of Dislocations and Plasticity," *Mechanics of Generalized Continua*, E. Kroner, ed. (Springer-Verlag, 1968), pp 269-278.

Newmark, N. M. and W. J. Hall, "Procedures and Criteria for Earthquake Resistant Design," *Building Practices for Disaster Mitigations*, BSS-46 (National Bureau of Standards, 1973).

Plummer, F. G., *A New Look at Structural Energy Dissipation*, Technical Report M-82/AD#780801 (CERL, May 1974).

Prager, W., "A New Method of Analyzing Stresses and Strains in Work-Hardening Plastic Solids," *Journal of Applied Mechanics*, Vol 23 (1956), pp 493-496.

Prager, W. and P. G. Hodge, *Theory of Perfectly Plastic Solids* (John Wiley, 1951).

Ramberg, W. and W. R. Osgood, *Description of Stress-Strain Curves by Three Parameters*, TN 902 (National Advisory Committee for Aeronautics, 1943).

Rice, J. R., "On the Structure of Stress-Strain Relations for Time-Dependent Plastic Deformation of Metals," *Journal of Applied Mechanics*, Vol 37 (1970), pp 728-737.

Valanis, K. C., "A Theory of Viscoplasticity Without a Yield Surface," *Archives Mechanics*, Vol 23 (1971), pp 517-551.

Ziegler, H., "A Modification of Prager's Hardening Rule," *Quarterly of Applied Mathematics*, Vol 17 (1959), pp 55-65.

APPENDIX A:

DERIVATION OF AN EXPRESSION FOR THE PARAMETER $d\mu$

The current stress state remains on the yield surface during plastic flow; therefore,

$$df^{(0)} = 0 \qquad \text{[Eq A1]}$$

where $f^{(0)}$ is given by Eq 1.

Eq A1 yields

$$\frac{\partial f^{(0)}}{\partial \sigma_{ij}} d\sigma + \frac{\partial f^{(0)}}{\partial a_{ij}^{(0)}} da^{(0)} + \frac{\partial f^{(0)}}{\partial \bar{\sigma}^{(0)}} d\sigma^{(0)} = 0 \qquad \text{[Eq A2]}$$

Partial differentiations of $f^{(0)}$ with respect to σ_{ij} and $a_{ij}^{(0)}$ are given by

$$\frac{\partial f^{(0)}}{\partial \sigma_{ij}} = -\frac{\partial f^{(0)}}{\partial a_{ij}^{(0)}} = P_{ij}^{(0)} \qquad \text{[Eq A3]}$$

From Eqs A2, A3, and 11

$$P_{ij}^{(0)} d\sigma_{ij} - P_{ij}^{(0)} d\mu(\sigma_{ij}^{q} - \sigma_{ij}) - \frac{2}{3} \bar{\sigma}^{(0)} d\bar{\sigma}^{(0)} = 0.$$

Therefore,

$$d\mu = \frac{P_{mn}^{(0)} \, d\sigma_{mn} + \frac{2}{3} \bar{\sigma}^{(0)} d\bar{\sigma}^{(0)}}{P_{ij}^{(0)} (\sigma_{ij}^{q} - \sigma_{ij})} \qquad \text{[Eq A4]}$$

APPENDIX B:

DERIVATION OF EQUATIONS OF INCREMENTAL PLASTICITY

From Eq 1, yield surface is given by

$$f^{(0)} = P_{ij}^{(0)} P_{ij}^{(0)} - \frac{2}{3}(\bar{\sigma}^{(0)})^2 = 0. \qquad \text{[Eq B1]}$$

Differentiation of Eq B1 with respect to σ_{ij} gives

$$\frac{\partial f^{(0)}}{\partial \sigma_{ij}} = P_{ij}^{(0)} \qquad \text{[Eq B2]}$$

From Eqs 15 and B2, the flow rule can be written as

$$d\varepsilon_{ij}^{p} = d\lambda P_{ij}^{(0)} \qquad \text{[Eq B3]}$$

Substitution of Eqs B2 and B3 into Eq 3 yields

$$(d\sigma_{ij} - c d\lambda\, P_{ij}^{(0)})\, P_{ij}^{(0)} = 0.$$

Therefore,

$$d\lambda = \frac{P_{ij}^{(0)}\, d\sigma_{ij}}{c\, P_{ij}^{(0)}\, P_{ij}^{(0)}} \qquad \text{[Eq B4]}$$

From Eqs B1 and B4

$$d\lambda = \frac{P_{ij}^{(0)}\, d\sigma_{ij}}{(2c/3)(\bar{\sigma}^{(0)})^2} \qquad \text{[Eq B5]}$$

To obtain $d\lambda$ in terms of strain increments $d\varepsilon_{ij}$, total strain increments are decomposed into their elastic and plastic components

$$d\varepsilon_{ij} = d\varepsilon_{ij}^{e} + d\varepsilon_{ij}^{p} \qquad \text{[Eq B6]}$$

From elastic constitutive equations, $d\sigma_{ij}$ is written as

$$d\sigma_{ij} = E_{ijkl}\, d\varepsilon_{kl}^{e} \qquad \text{[Eq B7]}$$

where E_{ijkl} are elastic coefficients.

From Eqs B6 and B7,

$$d\sigma_{ij} = E_{ijkl}\, (d\varepsilon_{kl} - d\varepsilon_{kl}^{p}) \qquad \text{[Eq B8]}$$

Eqs B3 and B8 yield

$$d\sigma_{ij} = E_{ijkl}\, (d\varepsilon_{kl} - d\lambda\, P_{kl}^{(0)}) \qquad \text{[Eq B9]}$$

By substituting $d\sigma_{ij}$ from Eq B9 into Eq B5 and rearranging terms, $d\lambda$ can be written as

$$d\lambda = \frac{P_{ij}^{(0)}\, E_{ijkl}\, d\varepsilon_{kl}}{(2c/3)(\bar{\sigma}^{(0)}) + P_{rs}^{(0)} E_{rstu}\, P_{tu}^{(0)}} \qquad \text{[Eq B10]}$$

$d\lambda$ from Eq B10 can now be substituted into Eq B9 to express $d\sigma_{ij}$ in terms of total strain components $d\varepsilon_{kl}$.

$$d\sigma_{ij} = \left[E_{ijkl} - \frac{P_{mn}^{(0)}\, E_{mnkl}\, E_{ijpq}\, P_{pq}^{(0)}}{(2c/3)(\bar{\sigma}^{(0)})^2 + P_{rs}^{(0)} E_{rstu} P_{tu}^{(0)}} \right] d\varepsilon_{kl} \qquad \text{[Eq B11]}$$

Material constant c used in Eqs B10 and B11 is obtained from a field of plastic tangent moduli as explained in Chapter 4.

CERL DISTRIBUTION

Picatinny Arsenal
ATTN: SMUPA-VP3

US Army, Europe
ATTN: AEAEN

Director of Facilities Engineering
APO New York 09403

DARCOM STIT-EDR
APO New York 09710

West Point, NY 10996
ATTN: Dept of Mechanics
ATTN: Library

Chief of Engineers
ATTN: Tech Monitor
ATTN: DAEN-ASI-L (2)
ATTN: DAEN-FEB
ATTN: DAEN-FESA
ATTN: DAEN-FEZ-A
ATTN: DAEN-MCZ-S
ATTN: DAEN-RDL
ATTN: DAEN-PMS (12)
for forwarding to
National Defense Headquarters
Director General of Construction
Ottawa, Ontario K1A0K2
Canada

Canadian Forces Liaison Officer (4)
US Army Mobility Equipment
Research and Development Command
Ft Belvoir, VA 22060

Div of Bldg Research
National Research Council
Montreal Road
Ottawa, Ontario, K1A0R6

British Liaison Officer (5)
US Army Mobility Equipment
Research and Development Center
Ft Belvoir, VA 22060

Airports and Const. Services Dir.
Technical Information Reference
Centre
KA0L, Transport Canada Building
Place de Ville
Ottawa, Ontario Canada K1A0N8

US Army R&S Group (Europe)
ATTN: AMXSN-E-RM
FPO NY 09510

Ft Belvoir, VA 22060
ATTN: Learning Resources Center
ATTN: ATSE-TD-TL (2)
ATTN: Kingman Bldg, Library

US Army Foreign Science & Tech Center
ATTN: Charlottesville, VA 22901
ATTN: Far East Office

Ft Monroe, VA 23651
ATTN: ATEN
ATTN: ATEN-FE-BG (2)

Ft McPherson, GA 30330
ATTN: AFEN-FED

USA-WES
ATTN: Concrete Laboratory
ATTN: Library

USA-CRREL

6th US Army
ATTN: AFKC-LG-E
I Corps (ROK/US) Group
I Corps (ROK/US) Group
ATTN: EACI-EN

US Army Engineer District
Saudi Arabia
ATTN: Library
New York
ATTN: Chief, Design Br
Buffalo
ATTN: Library
Pittsburgh
ATTN: Library
ATTN: Chief, Engr Div
Philadelphia
ATTN: Library
ATTN: Chief, NAPEN-D

US Army Engineer District
Baltimore
ATTN: Library
ATTN: Chief, Engr Div
Norfolk
ATTN: Library
ATTN: Chief, NAOEN-D
Huntington
ATTN: Library
ATTN: Chief, ORHED-D
Wilmington
ATTN: Chief, SAWEN-DS
Charleston
ATTN: Chief, Engr Div
Savannah
ATTN: Library
ATTN: Chief, SASAS-L
Jacksonville
ATTN: Library
ATTN: Const. Div
ATTN: Design Br, Structures Sec.
Mobile
ATTN: Library
ATTN: Chief, SAMEN-D
Nashville
ATTN: ORNED-D
Memphis
ATTN: Chief, LMMED-DT
Vicksburg
ATTN: Chief, Engr Div
Louisville
ATTN: Chief, Engr Div
Detroit
ATTN: Library
ATTN: Chief, NCEED-T
St. Paul
ATTN: Chief, ED-D
Chicago
ATTN: Chief, NCCED-DS
Rock Island
ATTN: Chief, NCRED-D
ATTN: Chief, Engr Div
St. Louis
ATTN: Library
ATTN: Chief, ED-D
Kansas City
ATTN: Library (2)
ATTN: Chief, Engr Div
Omaha
ATTN: Chief, Engr Div
New Orleans
ATTN: Library (2)
ATTN: Chief, LMNED-DG
Little Rock
ATTN: Chief, Engr Div
Tulsa
ATTN: Chief, Engr Div
ATTN: Library
Fort Worth
ATTN: Library
ATTN: Chief, SWFED-D
Galveston
ATTN: Chief, SWGAS-L
ATTN: Chief, SWGED-DS
Albuquerque
ATTN: Library
ATTN: Chief, Engr Div
Los Angeles
ATTN: Library
ATTN: Chief, SPLED-D
San Francisco
ATTN: Chief, Engr Div
Sacramento
ATTN: Chief, SPKED-D
Far East
ATTN: Chief, Engr
Japan
ATTN: Library
Portland
ATTN: Library
ATTN: Chief, DB-6
Seattle
ATTN: Chief, NPSCO
ATTN: Chief, EN-DB-ST
Walla Walla
ATTN: Library
ATTN: Chief, Engr Div
Alaska
ATTN: Library
ATTN: Chief, NPADE-R

US Army Engineer Division
Europe
ATTN: Technical Library
New England
ATTN: Library
ATTN: Chief, NEDED-T

US Army Engineer Division
North Atlantic
ATTN: Library
ATTN: Chief, NADEN-T
Middle East (Rear)
ATTN: MEDED-T
South Atlantic
ATTN: Chief, SADEN-TS
ATTN: Library
Huntsville
ATTN: Library (2)
ATTN: Chief, HNDED-CS
ATTN: Chief, HNDED-SR
Lower Mississippi Valley
ATTN: Library
Ohio River
ATTN: Library
ATTN: Chief, Engr Div
North Central
ATTN: Library
ATTN: Chief, Engr Div
Missouri River
ATTN: Library (2)
ATTN: Chief, MRDED-T
Southwestern
ATTN: Library
ATTN: Chief, SWDED-TS
South Pacific
ATTN: Chief, SPDED-TG
Pacific Ocean
ATTN: Chief, Engr
ATTN: FM&S Branch
ATTN: Chief, PODED-D
North Pacific
ATTN: Chief, Engr Div

Facilities Engineers
Ft Campbell, KY 42223
Ft Hood, TX 76544
FORSCOM
Ft Devens, MA 01433
Ft Lewis, WA 98433 (2)
Ft Carson, CO 80913
TRADOC
Ft Dix, NJ 08640
Ft Monroe, VA 23651
Ft Gordon, GA 30905
Ft Knox, KY 40121
Ft Sill, OK 73503
Ft Bliss, TX 79916
DSCPER
West Point, NY 10996
USAIC (2)
Ft Benning, GA 31905
USAAVNC
Ft Rucker, AL 36361
CAC&FL (2)
Ft Leavenworth, KS 66027
AMC
Dugway, UT 84022
USACE
Ft Huachuca, AZ 85613
HQ, 1st Inf Div & Ft Riley, KS 66442
HQ, 5th Inf Div & Ft Polk, LA 71459
HQ, 7th Inf Div & Ft Ord, CA 93941
HQ, 24th Inf & Ft Stewart, GA 31313

AF Civil Engr Center/XRL
Tyndall AFB, FL 32401

Little Rock AFB
ATTN: 314/DEEE (Mr. Gillham)

AFWL/DES
Kirtland AFB, NM 87117

Naval Air Systems Command
WASH DC 20360

NAVFAC/Code 04
Alexandria, VA 22332

Port Hueneme, CA 93043
ATTN: Library (Code L08A)

Washington, DC
ATTN: Building Research Advisory Board
ATTN: Transportation Research Board
ATTN: Library of Congress (2)
ATTN: Dept of Transportation Library

Defense Documentation Center (12)

Engineering Societies Library
New York, NY 10017